Theor Chim Acta (1995) 91: 225–236

Theoretica Chimica Acta

Bonding in C_2 and Be_2: Broken symmetry and correlation in DFT solutions

A. Goursot[1], J. P. Malrieu[2], D. R. Salahub[3]

[1] URA 418 CNRS, École de Chimie, 8 rue de l'École Normale, F-34053 Montpellier Cédex, France

[2] Laboratoire de Physique Quantique, URA 505 CNRS, Université Paul Sabatier, 118, route de Narbonne, 31062 Toulouse Cédex, France

[3] Département de Chimie, Université de Montréal, C.P. 6128, Succ. Centreville, Montréal (Qué), Canada H3C 3J7

Received May 1994/Accepted August 18, 1994

Summary. The solution of both Hartree–Fock (HF) and Kohn–Sham (KS) equations is based on the variational principle. Exact wavefunctions would obey the same symmetry restrictions contained in the total hamiltonian. However, the variational principle does not guarantee these symmetry restrictions and the HF and KS solutions are not necessarily symmetric in spin and space. Spatial and spin symmetry broken solutions with lower energies than their restricted analogues are examined for C_2 and Be_2, in the context of the KS formalism. Comparison with UHF solutions shows that KS instabilities are far less pronounced. The main differences between HF and KS solutions are related to effects of electron correlation.

Key words: Symmetry breaking – Correlation – DFI–HF instabilities

1 Introduction

The self-consistent solution of Hartree–Fock (HF) equations as well as that of Kohn–Sham (KS) equations is based on the variational principle, i.e. it requires that $\delta[E(D)] = \delta[\langle D|H|D\rangle/\langle D|D\rangle]$ is zero for an approximate Slater determinant D. If the system has symmetry properties, the exact wavefunction obeys the same symmetry restrictions contained in the total hamiltonian. However, the variational principle does not guarantee these symmetry restrictions and the HF or KS solutions are not necessarily symmetric in spin and space. If symmetry constraints are imposed in addition to the variational principle, the obtained symmetrical solution is then not necessarily the most stable one. Indeed, from its variation, $E(D)$ is stationary and represents an extremum in the variational space. However, only solutions for which this extremum is a minimum correspond to a so-called "stable" solution, which does not imply that it corresponds to the lowest energy. More stable solutions may be obtained through symmetry breaking in space and/or spin, which corresponds to the incorporation of single (and double) excitation effects into the Slater determinant.

The existence of broken-symmetry solutions in the context of HF equations was suggested in the 1950s [1–5]. After Thouless gave the mathematical stability conditions [6], unrestricted Hartree–Fock (UHF) theory was used extensively in

theoretical studies and applications. More details can be found in Fukutome's review article, which also contains a complete classification of all types of HF instabilities [7]. Applications of UHF theory to molecules (especially multiply bonded species) have shown how the use of broken symmetry orbitals leads to the incorporation of some amount of correlation into the single determinantal HF wavefunction [7–12]. These symmetry breakings reduce the unduly large fluctuations of the atomic charges imposed by the symmetry-adapted RHF solution and introduce part of the so-called left–right correlation. In multiple bonds, the spin unrestricted HF solutions also permit the alignment of the electron spins on the same atom and satisfy partly the atomic Hund rule. These effects prevail at large interatomic distance over the electronic delocalization and correct behaviours are then obtained.

Symmetry problems have also been given attention in density functional theory (DFT) [12–14]. In the standard KS formalism, different exchange-correlation potentials are used for spin-up and spin-down orbitals, resulting in a KS wavefunction which does not necessarily have the full symmetry of the exact solution (which would have been generated by the exact unknown exhange-correlation functional). The unrestricted Kohn–Sham (UKS) solutions are then not necessarily eigenfunctions of the total spin operator, although it has been recently demonstrated that, in the case of radicals, they are far less contaminated by higher spin states than their UHF counterparts [15].

It is also possible to formulate a restricted Kohn–Sham (RKS) theory in which the exact treatment of exchange and correlation would avoid any need for symmetry breaking: the exact RKS functional (which is clearly different from the exact UKS functional) would handle the proper electron correlation at every interatomic distance, yielding, for each electronic state, a total density with the proper symmetry.

A symmetrized KS formalism has been proposed recently, which deals with the density only (and not the spin density) and does not allow symmetry breaking [16]. The crucial point of its application depends on the availability of symmetry-dependent exchange-correlation functionals. The nature of these functionals remains to be determined.

It has been shown in previous DFT studies that broken-symmetry solutions may lead to reasonable results for molecular properties of diatomic molecules [17–19]. The broken-spatial symmetry problem for closed-shell molecules (analogous to a "singlet" type HF instability) can be solved by building a totally symmetric density from the average of the densities of the degenerate states with the same symmetry [14]. This can be achieved through DFT calculations with fractional occupation numbers, which corresponds in some sense to a configuration interaction between determinants with the same symmetry. Removal of the spin constraint for KS orbitals, which corresponds to a "non-singlet" type HF instability, has also been used in order to describe multiply bonded metal diatomics, among which Cr_2 has been a very famous example. These unrestricted calculations, which lead to different spin-up and spin-down orbitals, have been able to yield physical properties such as the bond length, vibrational frequency and dissociation energy in good agreement with experiment, whereas spin-restricted calculations could not.

There are other cases of strong instability for the symmetry-adapted RHF solution, which cannot be attributed to the left–right correlation in the bond but to the existence of low-lying valence virtual MO's of binding character. Double excitations to these MO's contribute largely to the wavefunction. In C_2 and Be_2 for instance, the σ system involves four electrons, which, at the RHF level, remain

essentially in 2*s* orbitals and repell. However, the $2p_z$ AO's are close in energy, defining a σ_g binding MO and specific non-dynamical (i.e. intra-valence) correlation occurs through excitations to that low-lying virtual MO. These effects induce dramatic symmetry-breakings of the HF wavefunction at *short* interatomic distances. The ability of density functional methods to treat correctly these specific intravalence near-degeneracy effects, inducing strong mixing of configurations with different space parts in the CI expansion, is a real challenge. It is thus interesting to see whether the symmetry-adapted KS solution is stable for such molecules. The use of symmetry-broken solutions at large interatomic distances in order to obtain a correct dissociation is acceptable, but their existence near the equilibrium is somewhat more problematic. Density functional calculations have already been devoted to these molecules at the local [17, 18, 20–22] and non-local [23, 24] levels.

The present study does not aim at the best possible description of the available physical properties of these molecules. Its purpose is (i) to compare HF and KS instabilities; (ii) to analyse how symmetry breaking in the context of UKS-DFT can handle the effects of correlation along the whole potential energy curve.

2 Details of the calculations

The results presented in this paper have been obtained with the program deMon [25, 26]. The non-local potential and energy functionals of Perdew and Yang for exchange [27] and Perdew for correlation [28] have been used during the SCF procedure. Although our purpose was not to focus on differences between various functionals, we have verified that other commonly used non-local expressions (i.e. Becke's for exchange and Perdew's 91 for exchange and correlation) lead to the same behaviour for the potential energy curves. No major difference was obtained for the equilibrium bond lengths and state energies. The potential energy curves displayed on Figs. 1 and 2 have been obtained using a DZVP basis set for C [29].

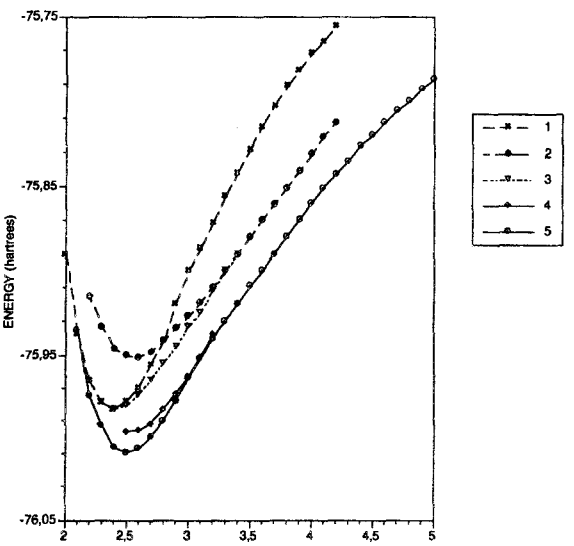

Fig. 1. Potential energy curves for the C_2 molecule: spin restricted KS solutions with physical contents: (1) $\sigma_g^2\ \sigma_u^2\ \pi_u^4$; (2) $\sigma_g^2\ \sigma_u^2\ \sigma'^2_g\ \pi_u^2$; (3) $\sigma_g^2\ \sigma_u^2\ \sigma_g'^x\ \pi_u^{4-x}$; (4) $\sigma^2\ \sigma^{*2}\ (s\ p_x\ p_y\ p_z)^2\ (s\ p'_x\ p'_y\ p'_z)^2$ to be compared with (5) $^3\Pi_u$ state

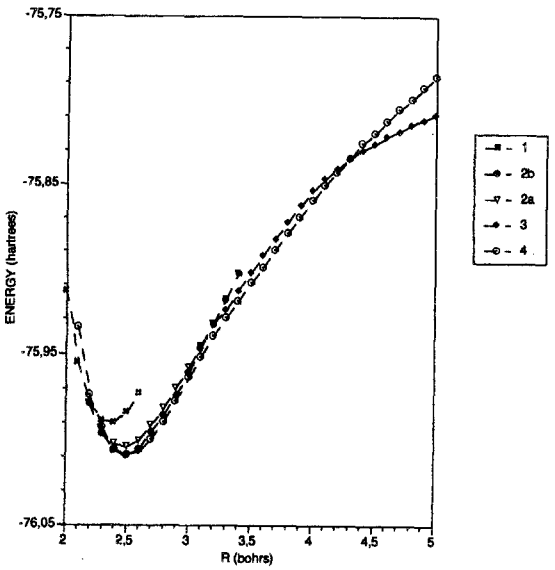

Fig. 2. Potential energy curves for the C_2 molecule: UKS solutions with physical contents (1) $\sigma\uparrow\ \sigma\downarrow\ \sigma^*\uparrow\ \sigma^*\downarrow\ (\pi_x^2)\uparrow\ (\pi_y^2)\downarrow$; (2a) $\sigma\uparrow\ \sigma\downarrow\ \sigma^*\uparrow\ \sigma^*\downarrow\ (\sigma'+\pi)\uparrow\ (\sigma'+\pi)\downarrow\ (\sigma''+\pi')\uparrow\ (\sigma''+\pi')\downarrow$; (2b) $\sigma\uparrow\ \sigma\downarrow\ \sigma^*\uparrow\ \sigma^*\downarrow\ (\pi_x\pi_y)\uparrow\ (\pi_x\pi_y)\downarrow\ (\pi_x'\pi_y')\uparrow\ \sigma'\downarrow$; (3) $\sigma\uparrow\ \sigma\downarrow\ \sigma^*\uparrow\ \sigma^*\uparrow\ \sigma^*\downarrow\ \sigma'\uparrow\ \sigma'\downarrow\ \pi_x\uparrow\ \pi_x\downarrow$; (4) $^3\Pi_u$ state

For C–C bond values between 2.4 and 2.8 bohr, a more extended basis set [30] has also been used, in order to check the effect of the basis set size on the equilibrium bond distances and energy minima of the lowest singlet and the $^3\Pi_u$ states. The corresponding points were all slightly stabilized with respect to the previous ones (by 0.10 eV), but the equilibrium bond distances and the relative energy difference between these two states were unchanged. The BSSE correction has been evaluated at 0.015 eV at the minimum. For Be_2 (Fig. 4), we have also used a DZVP basis set, taken from the Gaussian 92 package.

The numerical radial and angular integrations have been performed using a Gauss–Legendre integration scheme. After preliminary tests, a grid of 64 radial points and 98 angular points per radial shell has been chosen. However, for curve 4 in Fig. 1, a 242-point angular grid per radial shell was found to be necessary.

3 Results and discussion for the C_2 molecule

Experimentally, the C_2 molecule is known to have a $^1\Sigma_g^+$ ground state and a very low lying first excited $^3\Pi_u$ state, with an energy difference of 0.089 eV. All previous DF results lead to an erroneous $^3\Pi_u$ ground state, more stable by about 0.40 eV for LDA and 0.75 eV for non-local functionals [23]. The equilibrium bond distance and D_e values for the $^1\Sigma_g^+$ state are, however, in good agreement with experiment ($R_e = 2.349$ bohr, $D_e = 6.32$ eV [30]) for both local and non-local calculations.

Classically, the molecule in its ground state is described as having four electrons distributed in a π_u MO. The Hartree–Fock symmetry-adapted singlet solution, which can be described as $s_A^2\ s_B^2\ \pi_u^4$, is however not the most stable one at this uncorrelated level. A lower RHF singlet is found with a configuration $\sigma_g^2\ \sigma_u^2\ \sigma'^2_g\ \pi_u^2$ [11]. These two HF solutions have their minima near 2.40 and 2.60 bohr, respectively. The former solution is unbound with respect to the ground state atoms and the latter is bound by 1.20 eV. At the CASSCF level [32], the ground state is well described as a preponderant mixture of $\sigma_g^2\ \sigma_u^2\ \pi_u^4$ and $\sigma_g^2\ \sigma'^2_g\ \pi_u^4$

determinants with respective weights of about 70% and 15%. For C–C distances larger than 3.20 bohr, the $\sigma_g^2\,\sigma_u^2\,\sigma'^2_g\,\pi_u^2$ configuration is preponderant.

Potential energy curves obtained from previous spin-restricted DF results also show the crossing of the $^1\Sigma_g^+$ states, which correspond to the electronic $\sigma_g^2\,\sigma_u^2\,\pi_u^4$ and $\sigma_g^2\,\sigma_u^2\,\sigma'^2_g\,\pi_u^2$ configurations [17].

We have removed gradually the symmetry constraints, in order to understand the different effects of electron correlation, along the potential energy curve. First, the spatial symmetry constraint was removed, keeping a spin restricted scheme, and then, in a further step, all constraints were released.

4 Spin restricted calculations

The potential energy curves corresponding to the singlet spin-restricted calculations are presented in Fig. 1. For comparison, the triplet Π_u state (curve 5) is also reported. Curves 1 and 2 have been obtained using the D_{4h} subgroup of $D_{\infty h}$, the real symmetry of the C_2 molecule. Curve 1 refers to the $\sigma_g^2\,\sigma_u^2\,\pi_u^4$ configuration which corresponds to the experimental $^1\Sigma_g^+$ ground state. Its equilibrium bond distance is 2.38 bohr and its dissociation energy is 5.93 eV. Curve 2 is related to a $\sigma_g^2\,\sigma_u^2\,\sigma'^2_g\,\pi_u^2$ configuration, where the π_x and π_y orbitals are degenerate. This configuration corresponds to degenerate $^1\Sigma_g^+$ and $^1\Delta_g$ states. Its energy minimum lies at 2.60 bohr and it becomes the most stable singlet state at $R \geqslant 2.8$ bohr. These results are very comparable to previous local Xα calculations [17].

These two configurations differ by the occupations of their HOMO and LUMO orbitals (σ'_g and π_u), which vary with the C–C bond distance: π_u is more stable for $R \leqslant 2.2$ bohr, σ'_g more stable for $R \geqslant 2.8$ bohr and these two MO's are quasi-degenerate around the equilibrium geometry. As already proposed by Dunlap [14], it is possible to mix the densities corresponding to each of these configurations and to build a symmetrized total density yielding a solution which corresponds to a mixture of the two initial determinants. This can be achieved through the use of fractional occupation numbers. At each point R, an SCF calculation is performed allowing fractional occupations for the σ'_g and π_u orbitals (curve 3). There is no unique way to construct such a set of fractional occupation numbers. In our case, the fraction of electron transferred from the occupied to the virtual orbital was determined by the choice of a smearing parameter [25]. The optimal value for this parameter has been determined for each R value, in order to minimize the total energy (3-point-quadratic optimization).

As shown from Fig. 1, the mixture of the two configurations only occurs for distances $2.3 < R < 3.2$ bohr. For $R \leqslant 2.3$ bohr, a pure π_u^4 configuration describes the C–C bonding and for $R \geqslant 3.2$ bohr, the $\sigma'^2_g\,\pi_u^2$ configuration alone is sufficient to describe the C_2 electronic structure. The preponderant weight of this latter configuration for $R \geqslant 3.2$ bohr, is in complete agreement with CASSCF results [32].

If we compare the MO's obtained from our spin-restricted π_u^4 solution (curve 1) at $R = 2.4$ bohr with RHF results [11], we see that the main difference concerns the nature of the σ_g and σ_u valence MO's. For HF solutions, these MO's are mainly s-type lone pairs leading to a RHF solution of the form $s_A^2\,s_B^2\,\pi_u^4$. Our restricted KS results are different, since the σ_g and σ_u MO's are delocalized in s and p_σ orbitals, with a p_σ contribution of about 10% for σ_g and 16% for σ_u on each C atom. This electron delocalization is a result of the electron correlation which is included in DF calculations through the use of the exchange and correlation term. It is

worthwhile to compare with the CASSCF result at the same distance $R = 2.4$ bohr: the $\sigma_g^2\ \sigma_u^2\ \pi_u^4$ configuration is preponderant (71%) but completed with a contribution of about 13% of $\sigma_g^2\ \sigma_g'^2\ \pi_u^4$ configuration, which achieves the admixture of p_σ to s character. The weight of this latter configuration vanishes when R reaches 3.2 bohr, when the $\sigma_g^2\ \sigma_u^2\ \sigma_g'^2\ \pi_u^2$ configuration becomes preponderant [32]. Indeed, the KS orbitals at 3.2 bohr correspond to more localized s-type and p_σ-type MO's, since the p_σ contribution amounts to 5% for σ_g and 40% for σ_g', on each C atom. We can thus already conclude that the use of KS orbitals associated with the symmetrized broken-symmetry wavefunction leads to a good description of the evolution of the C–C bonding in the lower part of the potential energy curve.

We next investigated the possibility of another instability related to spatial symmetry alone and attempted to break the σ–π symmetry, keeping the two C atoms equivalent within a spin-restricted scheme. For this purpose, calculations have been performed in C_i symmetry, with trial densities identical for both C atoms and the requirement of identical alpha and beta orbitals. The use of a large random grid of points (around 15 000 points per atomic sphere) for the evaluation of the exchange-correlation terms was necessary. Its use allowed a new broken-symmetry solution to be obtained (curve 4, Fig. 1), at lower energies than the previous ones. Comparison with UKS solutions (Fig. 2) shows that this curve merges with them at around 3.0 bohr. For small R values, it should also merge with the lowest restricted solution (curve 1, Fig. 1) near 2.3 bohr, but it was technically impossible to obtain these points. The solutions represented by curve 4 correspond to broken σ–π MO's: the previous σ_g and π_u MO's remain combinations of s and p_z orbitals but the previous σ_g' and π_u MO's are now combinations of s, p_x, p_y, p_z orbitals. Although the σ–π symmetry has been broken, these solutions are spin-restricted since the alpha and beta orbitals are kept identical. In the R range where these spin-restricted solutions are available, the mixtures of s, p_x, p_y, p_z in the HOMO/LUMO change with R, in a very efficient way which lowers the total energy and allows the configurational change to be achieved easily.

5 Removal of the spin constraint

The lowest UHF solution of Σ^+ symmetry is about 2.5 eV below the lowest symmetry-broken RHF solution. It dissociates into a $^3P(S_z = 1)$C + $^3P(S_z = -1)$ C asymptote, i.e. in the UHF solutions of the atoms. However its physical content changes at short interatomic distances, the atomic spin population increasing near the equilibrium distance.

The Kohn–Sham analogue of an UHF solution may be obtained by performing spin-unrestricted calculations, starting from different alpha and beta densities. This has been achieved by starting from two triplet C atoms, with two spin-up electrons being localized on one C atom and two spin-down electrons on the other. Since the exchange and correlation terms are calculated by numerical integration over grid points, different solutions have been tried: no symmetry, C_i symmetry, cylindrical symmetry (treated as C_{4v}). In the following lines, the label σ is used for MO's containing s or/and p_z contributions and π for those which are built from p_x and/or p_y C orbitals. The spin-up and spin-down σ or π orbitals do not have necessarily the same spatial distribution.

Under these conditions, the complete potential energy curve of C_2 has been drawn, up to the dissociation limit. According to the value of the C–C distance, it is

possible to decompose the whole curve into three parts, which represent three groups of solutions (Fig. 2):

(a) For $R \geqslant 3.2$ bohr (curve 3): the asymptotic limit of two ^3P C atoms with a total atomic spin population (magnetic moment) of 2.0 is reached around 7.0 bohr. From large R values down to $R = 3.2$ bohr, the potential energy curve corresponds to a configuration of the type $\sigma\uparrow\ \sigma\downarrow\ \sigma^*\uparrow\ \sigma^*\downarrow\ \sigma'\uparrow\ \sigma'\downarrow\ \pi_x\uparrow\ \pi_x\downarrow$, comparable with the RHF configuration $\sigma_g^2\ \sigma_u^2\ \sigma_g'^2\ \pi_u^2$, at large distances. σ and σ^* have decreasing p_z contributions when R increases (6% at 3.2, less than 1% at 4.8 bohr), whereas σ' has an increasing p_z contribution (around 43% at 3.2 and almost pure p_z at 4.8 bohr).

(b) For $2.3 \leqslant R < 3.2$ bohr: when the 2 C atoms approach along z closer than around 3.2 bohr, the electron distribution among the alpha and beta MO's changes, leading to solutions where the σ–π symmetry has been broken. This is achieved for the solutions displayed on curves 2a and 2b. When the exchange and correlation contributions are evaluated through integration over the whole sphere for both C atoms and with no symmetry in the grid, the solutions which are obtained (curve 2a) correspond to a configuration $\sigma\uparrow\ \sigma\downarrow\ \sigma^*\uparrow\ \sigma^*\downarrow\ (\sigma' + \pi)\uparrow\ (\sigma' + \pi)\downarrow\ (\sigma'' + \pi')\uparrow\ (\sigma'' + \pi')\downarrow$, which can be considered as a Σ state. For $(\sigma' + \pi)$, the largest coefficients correspond to p_y and p_z orbitals, with small admixtures of s and p_x. The $(\sigma'' + \pi')$ spin-up and spin-down orbitals are mainly p_x contributions, with very small p_y and p_z coefficients. The calculated value of $\langle S^2 \rangle$ at the minimum is 0.94 showing that this solution is intermediate between a singlet and a triplet state. The $\langle S^2 \rangle$ values remain between 0.9 and 1.0 for the whole region $2.3 < R < 3.2$ bohr.

A different symmetry-broken solution (curve 2b), with a lower energy minimum, has also been obtained, through the use of C_{4v} symmetry (i.e. cylindrical symmetry) for the integration of the exchange and correlation terms (integration over the irreducible wedge and use of symmetry-adapted fitting functions). This solution corresponds to a configuration $\sigma\uparrow\ \sigma\downarrow\ \sigma^*\uparrow\ \sigma^*\downarrow\ (\pi_x\pi_y)\uparrow\ (\pi_x\pi_y)\downarrow\ (\pi_x'\pi_y')\uparrow\ \sigma'\downarrow$ and can be considered as a Π state. The calculated value of $\langle S^2 \rangle$ is 1.00 at the minimum and remains very close to this value in the $2.3 < R < 3.2$ bohr region.

For both solutions, the total atomic spin populations remain nearly equal to zero for these C–C distances. However, the MO contributions to the total atomic spin population are not equal to zero and have different values for the two above configurations.

The minima of curves 2a and 2b occur at 2.45 bohr, which is larger than the RKS minimum and too large with respect to the experimental value of 2.349 bohr. The corresponding binding energies are 6.55 eV (curve 2a) and 6.62 eV (curve 2b).

(c) For $R < 2.3$ bohr (curve 1): the SCF solution changes to a $\sigma\uparrow\ \sigma\downarrow\ \sigma^*\uparrow\ \sigma^*\downarrow\ (\pi_x^2)\uparrow\ (\pi_y^2)\downarrow$ form comparable to the RKS solution at short distances. At 2.2 bohr, the calculated value of $\langle S^2 \rangle$ is 0.70.

These different broken symmetry solutions merge into a complete potential energy curve which describes the transformation of the C_2 electronic structure as a function of the C–C bond distance. It is worth noting that the energy minima of both Σ and Π solutions are very close to that of the $^3\Pi_u$ state (minimum at 2.50 bohr, experimental value at 2.48 bohr). The Π-type "singlet" is degenerate with the triplet state and the Σ-type "singlet" is calculated to be 0.09 eV higher in energy.

It is interesting to analyse the variation of the total atomic spin population as a function of R and to compare it with UHF results (Fig. 3). As expected, the atomic spin population amounts to 2.0 at the dissociation limit. It decreases regularly to zero when the two C atoms approach each other, reaching a zero value

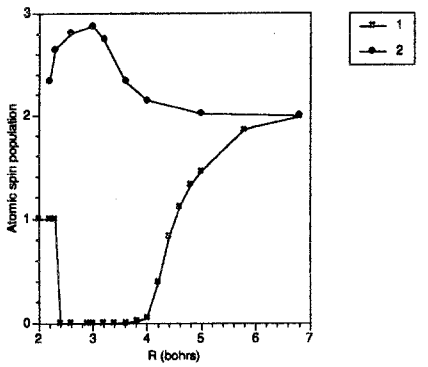

Fig. 3. Evolution of the atomic spin population of the C_2 molecule: (1) UKS solution; (2) UHF solution (reproduced from Ref. [11])

Table 1. Be_2 molecule: Mulliken population for atom A (α spin and total electronic population) for the unrestricted-spin solution at four interatomic distances

R in bohr	s Population (except 1s)		p_z Population		Total atomic spin population		
	α-spin	Total	α-spin	Total	s	p_z	Total
3.8	0.847	1.470	0.420	0.530	0.224	0.310	0.534
4.5	0.900	1.696	0.227	0.304	1.104	0.150	0.254
5.0	0.911	1.805	0.108	0.195	0.017	0.021	0.038
5.4	0.931	1.861	0.070	0.140	0.001	0.000	0.001

($\leqslant 0.005$) around 3.5 bohr. This decrease is very rapid near 4.0 bohr. When the total spin population is negligible, each spin orbital is distributed quasi-equally among the two C atoms, but the spin-up and spin-down orbitals differ spatially. When symmetry is imposed in a spin-restricted scheme, the spin density is zero for each MO (same spatial part for alpha and beta spin orbitals), leading to a zero value for $\langle S^2 \rangle$. For the broken symmetry solution, the minimum of the curve corresponds indeed to equal total $\rho\uparrow$ and $\rho\downarrow$ populations, but differently distributed through space since the s, p_π and p_σ contributions to these spin-up and spin-down populations are not equal. In the C–C region where the total spin population is zero and $\langle S^2 \rangle$ is close to 1.0, there is, for each atom, a compensation between spin-up and spin-down contributions. At short ($\leqslant 2.3$ bohr) or large ($\geqslant 3.5$ bohr) distances, these two contributions do not compensate.

This description is very different from the lowest UHF solution [11], which corresponds, in the equilibrium distance region, to two ^5S C atoms, coupled together with a resulting spin population close to 3 at 2.4 bohr (Fig. 3).

These results show that the first stabilizing effect of spatial broken symmetry is to account for more non-dynamical correlation effects through the mixing of s, p_x, p_y p_z contributions (curve 4, Figs. 1 and 2). We can say that this solution mimics a multideterminantal approach, in which dynamical correlation effects would have also been included. The spin-symmetry breaking, which introduces spin fluctuations into atomic orbitals, allows the C_2 bonding to be stabilized further. This stabilization could be expressed in a CI language as contributions to the bonding of other C configurations like $s^2\ p_x\uparrow\ p_z\downarrow$, $s\uparrow\ p_x\downarrow\ p_y\downarrow\ p_z\uparrow$ or $s\uparrow\ p_x\downarrow\ p_y\downarrow\ p_z\downarrow$.

6 Results and discussion for the Be_2 molecule

Be_2 has a very weak bond energy of 0.1 eV [33] but a rather short bond distance of around 4.6 bohr. RHF calculations yield no bonding and only very well correlated calculations are able to account for a bond between the two $1s^2\ 2s^2$ Be atoms [34–36]. Density functional results lead to a reasonable bonding energy, especially at the nonlocal level [24]. The π-type LUMO of the Be dimer is substantially higher in energy than the σ-type HOMO (1.62 eV) and, therefore, in contrast to C_2, the $^1\Sigma_g^+$ ground state is the only low-lying singlet state. We have thus only investigated spin-symmetry breaking, in comparison with the spin-restricted solution.

The potential energy curve obtained for the spin-restricted symmetry-adapted solution (curve 1, Fig. 4) displays a minimum at 4.6 bohr and the corresponding dissociation energy is 0.38 eV. This curve corresponds to solutions of the form $s_A^2\ s_B^2\ \sigma_g^2\ \sigma_u^2$. This solution dissociates correctly into ^1S Be atoms.

The σ_g and σ_u MOs contain a non-negligible p_σ character: the p_σ orbital participates for 6% in σ_g and 10% in σ_u, for each Be atom, which means a population of 0.32 p_z electron per atom (the s population being of 1.68 electron per atom). As for C_2, this result is different from the RHF solution which yields essentially s-type MO's, leading to a purely repulsive interaction between the two Be atoms [11].

However it should be mentioned that a binding potential energy curve is obtained in the UHF formalism. The UHF solution is always lower than the RHF one, even at infinite distances, since the Be RHF solution $|1s^2\ 2s^2|$ is unstable. For the Be atom, the UHF solution puts the valence α and β electrons in different orbitals accepting 2_{Pz} components of opposite amplitude ($\sigma\uparrow = 2s\uparrow + 2p_z\uparrow$; $\sigma\downarrow = 2s\downarrow - 2p_z\downarrow$), which introduces a small amount of angular correlation. Notice that this instability disappears in the KS formalism. At short interatomic distance, the energy gain obtained by the release of the spin constraint is much larger, and the UHF wavefunction, in the minimum region, may be described as involving a large contribution of a $^3P(S_z = 1)\text{Be}^* + {}^3P(S_z = -1)\text{Be}^*$ interaction since the atomic spin becomes important. In view of this strong UHF symmetry breaking, it is interesting to see whether the restricted KS solution is stable.

If we use atomic ^3P densities as trial solutions (corresponding to the excited $1s^2\ 2s\uparrow\ 2p\uparrow$ atomic configuration) to start the SCF procedure, UKS solutions are obtained (curve 2, Fig. 4). This potential energy curve remains close to the spin-restricted one for Be–Be distances lower than 4.8 bohr and merges with it for larger R values. At distances shorter than 4.6 bohr, this solution has a form $s_A^2\ s_B^2\ \sigma^2\ \sigma'^2$ with a non-zero spin density on each Be atom. The energy minimum occurs at a shorter distance than the restricted curve (4.48 bohr), with a slightly larger binding energy of 0.40 eV. As shown in Table 1, the total atomic spin density decreases from 0.5 at 3.8 bohr to a zero value at 5.0 bohr. At very short distances, the p_σ contribution to the occupied MO's is large (0.53 electron at 3.8 bohr). Moreover, the total atomic spin population is more concentrated on the p_σ (0.310) than on the s orbital (0.224). In fact, the antibonding σ' MO has a more pronounced p_σ character than the bonding σ MO and its contribution to the atomic spin population is the dominant one.

When R increases, the p_σ contribution to the σ MOs decreases, reaching the value obtained for the spin-restricted calculations at R values close to 4.5 bohr. However, the total atomic spin population is still non-vanishing, mainly due to

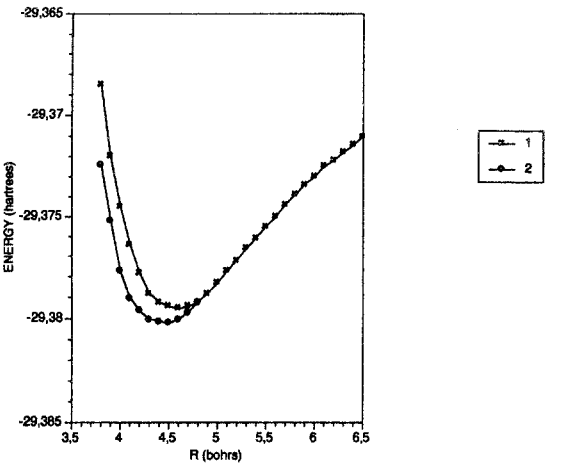

Fig. 4. Potential energy curves for the Be_2 molecule: (1) RKS solution; (2) UKS solution

the σ' MO. At R values larger than 4.5 bohr, the atomic spin density vanishes very rapidly, and the potential energy profile joins the spin-restricted curve.

Comparison with UHF results shows that the UKS solution displays the same tendencies, although with less extreme features:
– the total atomic spin population goes from zero at large distance to a non-negligible value (0.25) at the equilibrium bond distance, but this value is twice as large for the UHF solution.
– the p orbital has a more pronounced spin density than the s orbital.
– the p population grows when the interatomic distance decreases, but its value amounts to 0.3 electron at the minimum compared with 0.6 electron in UHF.

As for C_2, the main difference between RHF and RKS results corresponds to the presence of non-dynamical correlation in DF solutions. This enables restricted KS solutions to handle the effects of the $2s$–$2p$ correlation. Although the difference between the unrestricted and restricted curves is small with respect to the HF analogues [11], the UKS curve reveals the existence of an instability, related to some admixture of ^3P Be contributions.

7 Conclusions

The C_2 and Be_2 examples have shown that the KS solutions, which are obtained variationally as are the HF solutions, do not display the same dramatic instabilities. The huge differences between RHF and UHF solutions are not reproduced in DFT. Indeed, the 3.7 eV difference between the RHF and UHF minima for C_2 is decreased to 0.75 eV in the case of KS calculations. For Be_2, the contrast is even larger, since the RHF solution is repulsive whereas the RKS and UKS results are very close.

Electron correlation makes the major difference between HF and KS solutions at the restricted level. Electron correlation may be traditionally separated into dynamical and non-dynamical (or internal) correlation [37]. Density functional methods, using exchange and correlation potentials derived from the free electron gas include dynamical correlation effects, in contrast to Hartree–Fock theory. Moreover, the symmetry constrained RHF solution does not display any $2s$, $2p_z$

mixing in the σ MO's of C_2 and Be_2. However, this mixing already occurs in the restricted KS solution, showing the existence of "internal" correlation effects, which can only be obtained from spatial and/or spin symmetry breaking in HF [11] or, through the use of several determinants [32]. Spatial σ–π symmetry breaking is also a way to recover more internal correlation.

The spin symmetry breaking plays the same role in UHF and UKS, bringing in correlation through mixtures with other atomic configurations. However, the UHF and UKS solutions are very different, because the antiferromagnetic character is far less pronounced in the DF results, with a substantially smaller contamination of high spin multiplets. Although one might have expected a break-down of the UKS method for cases like C_2 and Be_2 where nondynamical correlation plays such an important role, such is not the case. Of course, the results are not fully satisfactory since the symmetry of the ground state still remains incorrect for C_2 and since the binding energy of Be_2 is about four times too large. However the KS symmetry breakings are of a much smaller amplitude than the HF ones and do not produce irrealistic potential energy curves.

Symmetry breaking in DFT can thus be considered as a way to gain a better description of electron correlation effects. This study has shown that this description is not completely satisfactory, due to the approximate nature of the XC potential. The exact unknown UKS-XC functional would lead for C_2 to a GS of the proper symmetry ($^1\Sigma_g^+$). Since we are not using this exact functional, errors in the relative stabilities of molecular states may occur. Moreover, for UKS solutions, the symmetry of the total density may not be exact in every region of space, corresponding to a lack of symmetry in the total wave function.

References

1. Slater JC (1951) Phys Rev 82:538
2. Coulson CA and Fischer I (1949) Phil Mag 40:386
3. Löwdin PO (1954) Proceedings of the Nikko symposium on molecular physics (1953) Maruze, Tokyo, p 13
4. Löwdin PO (1955) Phys Rev 97:1509
5. Löwdin PO (1963) Rev Mod Phys 35:496
6. Thouless DJ (1961) The quantum mechanics of many body systems. Academic Press, NY
7. Fukutome H (1981) Int J Quantum Chem XX:955
8. Mayer I (1978) Int J Quantum Chem XIV:29
9. Cook DB (1986) J Chem Soc Faraday Trans 2:187
10. Lepetit MB, Malrieu JP, Pélissier M (1989) Phys Rev A39:981
11. Lepetit MB, Malrieu JP (1990) Chem Phys Lett 169:285
12. Dunlap BI (1987) Adv Chem Phys 69:287
13. Dunlap BI (1988) Chem Phys 125:89
14. Dunlap BI (1991) in: Andzelm J, Labanowski J (eds) Density functional methods in chemistry. Springer, Berlin, p 49
15. Baker J, Scheiner A, Andzelm J (1993) Chem Phys Lett 216:38; Eriksson LA, Malkina OL, Malkin VG, Salahub DR (1994) J Chem Phys 100:5066
16. Görling A (1993) Phys Rev A 47:2783
17. Dunlap BI, Mei WN (1983) J Chem Phys 78:4997
18. Dunlap BI (1984) Phys Rev A29:2902
19. Baykara NA, McMaster BN, Salahub DR (1984) Mol Phys 52:891
20. Harris J, Jones RO (1979) J Chem Phys 70:830
21. Jones RO (1979) J Chem Phys 71:1300
22. Painter GS, Averill FW (1982) Phys Rev B26:1781

23. Kutzler FW, Painter GS (1992) Phys Rev B45:3236
24. Murray CW, Handy NC, Amos RD (1993) J Chem Phys 98:7145
25. St-Amant A, Salahub DR (1990) Chem Phys Lett 169: 387; St-Amant A Thesis (1992), Université de Montréal.
26. Daul CA, Goursot A, Salahub DR (1993) In: Leforestier C (ed.) Proceedings NATO ARW on Grid methods in atomic and molecular quantum calculations. Kluwer Academic Publishers, Doredrich, p 153
27. Perdew J, Yang Y (1986) Phys Rev B33:8800
28. Perdew J (1986) Phys Rev B33:8822
29. Andzelm J, Salahub DR (1987) In: Jena P, Rao BK, Khanna SN (eds) Physics and chemistry of small clusters, Nato Advanced Study Institute, Physics, Plenum, New York, Vol 158, p 867
30. van Duijnevelt-van de Rijdt JGCM, van Duijnevelt FB (1982) J Mol Struct Theochem 89:185
31. Huber KP, Herzberg GH (1979) Constants of diatomic molecules. Van Nostrand Reinhold, NY
32. Kraemer WP, Roos BO (1987) Chem Phys 118:345
33. Bondybey VE, English JH (1984) J Chem Phys 80:568
34. Liu B, McLean AD (1980) J Chem Phys 72:3418
35. Harrison RJ, Handy NC (1986) Chem Phys Lett 123:321
36. Petersson GA, Shirley WA (1990) Chem Phys Lett 160:494
37. Sinanoglu O (1969) Adv Chem Phys 14:237